544.45

Study on ignition of high energy material with aluminum and metal powders

A.G. Korotkikh[1], V.A. Arkhipov[2], K.V. Slyusarskiy[1], I.V. Sorokin[1]

[1]Tomsk polytechnic university, 634050 Tomsk

[2]Tomsk state university, 634050 Tomsk

korotkikh@tpu.ru

1. Introduction

Boron is one of the most promising metals for rocket fuels due to high specific combustion heat value (among the highest per unit of mass and the maximum possible per unit of volume [1]). However, its application is significantly complicated by the fact that inert layer of boron is formed on the surface of boron particles during storage and combustion. It prevents the access of oxidizer [2] to pure boron, significantly reduces the activation energy of the boron combustion reaction (by 25 kJ / mole according to [3]) and increases the density of the fuel [4].

Devoted to the investigation of boron oxidation processes articles are mainly represented in literature by three types of works: the study on the oxidation of single particles [5, 6] and boron powders [7-10], as well as boron-containing composite fuels [11, 12].

The mechanism of ignition and combustion of single particles and boron powders in an oxidizing medium has been studied in sufficient detail. The overall exothermic burning reaction of a boron particle in an oxygen medium can be represented in the form [13]:

$$2B + 2O \rightarrow B_2O_2$$

Two modes are distinguished for single boron particle burning: low-temperature heterogeneous combustion [14] and high-temperature homogeneous gas-phase combustion [14].Considering the sufficiently high boiling point of boron oxide (2316 K [1]), two stages are additionally separated out in the low-

temperature mode: evaporation of the boron oxide film (at this stage, the rate of the oxidation reaction is determined by the rate of oxidant diffusion to the particle) and heterogeneous oxidation of boron (at this stage overall oxidation rate is determined by the rate of chemical reaction [4]). It is established that with increasing pressure the delay times of boron particles ignition [5] are reduced according to the power law, while the boron ignition temperature does not depend on the oxidizer partial pressure [5]. At the same time, the dependence of the ignition delay time on the particle size is linear [10]. Since in the kinetic regime the rates of chemical reactions are small, generated during reaction heat is dissipating into the environment without a significant increase in the temperature of the medium. This process is not self-sustaining and of limited practical interest. Since the boron oxidation products are non-volatile at temperatures below 2316 K, an oxide layer forms in the boron surface during heating. The melting point of boron oxide is 450 ° C, so oxygen diffuses through the melted layer when temperature rises above point, while pure boron dissolves in it further accelerating the combustion process [13]. Oxide layer affects the ignition of boron particles by increasing ignition delay time and temperature [2]. Increasing particle size causes increasing of the oxide layer thickness [2] and temperature gradients. It also has a negative effect on the ignition and combustion parameters [10]. At higher temperatures (of the order of 2500 K [3]), the combustion mechanism changes to a gas phase. Then incomplete oxides of boron evaporate and combustion occurs in the gas phase, but such regimes are rarely obtained in practice. Relatively high ignition delay times of the boron powder produced by the electrodispersion method with particle size less than 10 μm [9] – 80 ms. Time of complete combustion is long enough too, which makes it difficult to use in practice. To improve combustion parameters, powder additives of metals and their oxides are used [6, 7]: magnesium, aluminum, bismuth, cerium, iron, copper. This makes it possible to reduce the ignition delay times of powders up to 2x times [6] and the ignition temperature up to 10% (up to 685 ° C) [12]. The introduction of such additives also makes it possible to increase the completeness

of conversion [6-8]. Altogether, it makes the use of bimetallic powders one of the most promising directions of research.

The most widespread application for boron powders is in the sphere of composite fuels [1]. Because in such systems the oxidant has the same phase as the fuel, the mechanism of their combustion differs significantly from described above. As solid oxidant the following substances may be used [4, 3]: polybutadiene (HTPB), ammonium perchlorate (NH_4ClO_4), potassium perchlorate ($KClO_4$),hexanitrohexaazaisowurtzitane (CL-20), lithium perchlorate ($LiClO_4$), potassium nitrate (KNO_3). Numerous studies presented in literature on the characteristics of boron propellants ignition and combustion with different particle size [15], binder (most commonly used NH_4ClO_4, KNO_3) [3, 4] and the ratio of fuel to oxidizer [13, 16]. CO_2–continuous laser is used to initiate the combustion of fuels in studies designed to investigate flame spectral parameters and determine characteristic temperatures [2, 3, 4, 16]. It is worth mentioning, that in all these studies are carried out at atmospheric pressure. In studies aimed at studying combustion at high pressures [17] or under conditions close to real ones [1, 13, 17] the conductive initiation (for example, heating with nichrome filament [17] or hot gases in TGA chamber [6, 7]) was used. It was established that with an increase in the pressure and content of boron particles in the fuel, the linear burning rate and the surface temperature of the sample increase [3] with the pressure dependence form close to linear [18]. Compared to the combustion of single boron particles, the correlation coefficient value is higher, which may be due to an increase in the thermodynamically equilibrium fraction of the condensed combustion products in reaction products. It leads to a reduction in two-phase losses [1]. Because of the much greater variety of substances and elements in such systems (in comparison with the combustion of single metal particles), the reaction mechanism is much more complicated and studied not so well. The main reactions in the combustion of metals with a solid oxidizer in the form of perchlorate are the oxidation of boron and the decomposition of perchlorate [19]:

$$2KClO_4 + 2B = 2KBO_3 + Cl_2 + 2O_2$$

$$KClO_4 = KCl + 2O_2$$

Various techniques have been used to improve the characteristics of composite boron-based fuels. The one popular solution is using of coatings [3] to prevent the formation of an oxide film, another is using bimetallic powders [20] with an ignition temperature of second metal lower than the evaporation temperature of the boron oxide film.

In this paper, we present the results of the experimental study on ignition delay times and corresponding surface temperature of solid ammonium perchlorate-based fuel samples with various types of boride powders. The study was carried out using a laser of continuous action.

2 Experimental section

2.1 Sample characterization

Five HEM samples were used for ignition delay time definition experiments. The first is the basic composition of HEM, containing ammonium perchlorate (PCA) (fraction 160-315 μm), ammonium nitrate (NA) (fraction less than 50 μm), active fuel-binder MPVT-ASP and metal fuel - microsized aluminum powder ASD-4 (30% by weight). Other four formulations of HEM aluminum powder is completely substituted by boron powders B, aluminum diboride AlB_2, aluminum dodecaboride AlB_{12} and titanium diboride TiB_2.

2.2. Experimental setup

HEM ignition process was carried out using setup based on the CO_2 laser of continuous action with a wavelength of 10.6 microns and a maximum power of 200 W (Fig. 1). HEM samples were cut into 5 mm high tablets before the experiment. The flat end surface of the samples was visually monitored for the absence of pores, cavities and cracks.

The test sample (6) of the HEM was attached to the holder (8). When the shutter (4) was opened, the heat flux was directed to the investigated HEM sample (6). The signals from the photodiodes (7) were transmitted through the L-card E-14-440 ADC (9) and recorded using personal computer (10), and then processed using the LGraph2 software. The ignition delay time t_{ign} of HEM was defined as a

difference between the time of signal from photodiodes (7), one of which registered the occurrence of flame on the flat end surface of the sample. Relative error for delay time values t_{ign} was 5-12% with confidence level 0.9.

The surface temperature of the fuel sample during the heating was recorded using a Jade J530 SB thermal imaging camera at a frequency of 50 Hz in the temperature range 373-1800 ° C. The thermal imaging data and the photodiode parameters were synchronized by a characteristic click produced by shutter opening. It corresponds to the beginning of the HEM sample heating.

The power of the laser radiation heat flux on the HEM sample was measured with a thermoelectric sensor Ophir FL400A (3). A maximum value of the radiation power at the center of the laser beam was determined through 2 mm diameter diaphragm.

2.3 Activation energy calculation

The activation energy value was determined by solving the inverse heat conduction problem of the heated by radiant flux sample according to the given in [21] method. It is based on the following equation:

$$\lg\left(\frac{t_{ign}}{\left(1-T_0/T_*\right)^2}\right)=\lg\left(\frac{0,349\cdot Ec}{\left(1-0,8\cdot\beta\right)R\cdot Qz}\right)+\frac{E}{RT_*}\lg(e)$$

here t_{ign} - experimentally determined ignition delay time, s; T_0 - initial temperature of solid fuel sample, K; T_* - characteristic temperature of solid fuel sample, K; E - effective activation energy of the reaction, J / mole; c - specific heat of the solid fuel sample, J / (kg K); $\beta = RT_* / E$ - unit less parameter which expresses the degree of dependence of the reaction rate on temperature; R - universal gas constant, J / (mole K); Q - the thermal effect of the reaction, J / kg; z - reaction pre-exponent, 1 / s.

The value of the characteristic temperature can be determined by the following formula:

$$T_* = T_н + \sqrt{\frac{t_з\cdot\left(1-0,8\cdot\beta\right)}{0,698}}\cdot q_s$$

Here q_s - flux density, W / cm^2.

3 Results and discussion

3.1 Ignition delay time

The dependence of the ignition delay times of solid fuel samples on the radiation flux density were obtained using setup for radiant heating. These dependences are shown in fig. 2.

The graph in fig. 2 shows that a complete replacement of the ASD-4 aluminum powder with boron powder results in a decrease in the ignition delay time of solid fuel samples by 2.2-2.8 times.The use of aluminum borides makes it possible to reduce the ignition delay time of fuels in comparison with the base composition by 1.7-2.2 times. Differences in the ignition delay times for titanium borides from the base sample differ slightly, by 10-25%. An analysis of these results shows that the ignition delay of fuel samples heated by a radiant flux depends on the combustion heat of metal additives. The worse characteristics of composite fuel based on industrial aluminum ASD-4 are explained by the high average particle size in the comparison with other samples.

The experimental dependences obtained were approximated by a power function of the following form:

$$t_{ign} = A \cdot q^{-B}$$

here t_{ign} - solid fuel ignition delay time, s; q - heat flux density, W / m^2; A, B - approximation constants.

Approximation constant and determination coefficient R^2 values for experimental data are given in Table 1.

3.2 Ignition temperature

Figure 3 shows the synchronized video frames and thermogramms corresponding to the main stages of ignition on an example of HEM sample with metal AlB_2 additive.

Results of thermal imaging of fuel samples at the time corresponding to the ignition are shown in Fig. 4. Based on the analysis of the presented in Fig. 4 data,

the characteristic surface temperatures of the HEM samples were obtained at the time corresponding to the fuel ignition. The temperatures are shown in Table 2.

It is worth mentioning, that the maximum and average temperatures of sample ignition with aluminum boride and pure boron powders are fairly close. This may indicate the leading role of the boron oxidation reaction during ignition.

Obtained experimental dependences of maximum and average temperatures over the cross section surface on time are shown in figs. 5 and 6, respectively.

The graphs in figs. 5 and 6 show that the process of heating and ignition of composite fuel can be divided into two stages with different rates of surface temperature increasing. This can be caused by an increased rate of exothermic reactions at higher temperatures.

The slope of the temperature curves in the first stage is generally due to conductivity of samples. In this case, the average temperature of the sample surface is most indicative – fig. 6. From the slope of the curves, it can be concluded that the conductivity of all fuels is at approximately same level, i.e. the type of metal addition practically does not affect the stage of fuel heating.

The slope angle for the second stage is related to two factors - the rate and the thermal effect of the exothermic reaction. Taking into account that boron has the highest specific heat of combustion, it can be concluded that the rate of reactions for compositions containing aluminum boride powders is substantially higher than for pure boron.

3.3 Effective activation energy

Using presented in section 2.3 methodology, effective activation energy and the ignition temperature of the solid fuel samples was determined, calculation results are shown in table 3.

According to table 3, samples with the AlB_{12} additive have the highest activation energy, while for samples with AlB_2 it is the lowest. Based on these data it can be concluded that the addition of AlB_2 into composition of HEM is preferred.

4 Conclusion

Experimental studies on ignition of the five solid fuel compositions based on ammonium perchlorate with additives of metal powders ASD-4, B, AlB_2, AlB_{12} and TiB_2 by continuous laser radiation. Ignition delay times for all the samples in the heat flux density range of 90-200 W/cm^2 were determined. The lowest values of ignition delay times in all regimes were recorded for samples with the addition of pure boron B, while the highest values were obtained for a standard sample with ASD-4. Using the thermal imaging data, the ignition temperatures of these fuels were determined, as well as the dependence of the mean and maximum surface temperature of the sample on time. Analysis of the time dependences on temperatures shows that the rate of oxidation of samples containing aluminum borides exceeds the rate of oxidation of samples with pure boron. Analysis of the initial stage of powder oxidation allows to say that the formation of an oxide film does not occur during ignition of composite fuels Activation energy values of ignition process were defined for investigated composite fuels. The lowest activation energy value was obtained for fuels with the aluminum boride AlB_2 additive (97.51 kJ / mole), the highest - with the aluminum dodecaboride AlB_{12} (306.9 kJ / mole).

Bibliography:

1. Gany A., Timnat YM Advantages and drawbacks of boron-fueled propulsion // Acta Astronautica. - 1993. ¬ V. 29, No. 3. - P.181-187.

2. Ao W., Wang Y., Li H., Xi J., Liu J., Zhou J. Effect of Initial Oxide Layer on Ignition and Combustion of Boron Powder // Propellants, Explosives, Pyrotechnics. - 2014. - V. 39. - P. 185-191.

3. Liang D., Liu J., Chen B., Zhou J., Cen K. Improvement in energy release properties of boron-based propellant by oxidant coating // Thermochimica Acta. - 2016. - V. 638. - P. 58-68.

4. Liang D., Liu J., Xiao J., Xi J., Wang Y., Zhang Y., Zhou J. Energy release properties of amorphous boron and boron-based propellant primary combustion products // Acta Astronautica. - 2015. - V. 112. - P.182-191.

5. Foelsche RO, Burton Rl, Krier H. Boron Particle Ignition and Combustion at 30-150 ATM // Combustion and Flame. - 1999. - V. 117. - P.32-58.

6. Xi J., Liu J., Wang Y., Hu Y., Zhang Y., Zhou J. Metal Oxides as Catalysts for Boron Oxidation, Journal of Propulsion and Power. - 2014. - V. 30, No. 1. - P. 47-53.

7. Liu JZ., Xi JF., Yang WJ., Hu YR., Zhang YW., Wang Y., Zhou JH. Effect of magnesium on Actual Characteristics of boron particles // Acta Astronautica. - 2014. - V. 96. - P.89-96.

8. Liu LJ., He GQ., Wang YH. Thermal reaction characteristics of the boron used in the fuel-rich propellant // Journal of thermal analysis and calorimetry. - 2012. - V. 114, I. 3. - P.1057-1068.

9. Jain A., Josepha K., Anthonysamy S., Gupta GS Kinetics of oxidation of boron powder // Thermochimica Acta. - 2011. - V. 514. - P.67-73.

10. Jain A., Anthonysamy S., Ananthasivan K., Gupta GS Studies on the ignition behavior of boron powder // Thermochimica Acta. - 2010. - V. 500. - P.63-68.

11. Kuwahara T., Kubota N. Role of Boron in the Burning Rate Augmentation of AP Composite Propellants // Propellants, Explosives, Pyrotechnics. - 1989. - V. 14. - P.43-46.

12. Ulas A., Risha GA, Kuo KK An Investigation of the Performance of a Boron / Potassium-Nitrate Based Pyrotechnic Igniter // Propellants, Explosives, Pyrotechnics. - 2006. - V. 31, No. 4. - P.311-317.

13. Ulas A., Kuo KK, Gotzmer C. Ignition and Combustion of Boron Particles in Fluorine-Containing Environments // Combustion and Flame. - 2001. - V. 127. - P.1935-1957.

14. Mohan G., Wlliams FA Ignition and Combustion of Boron in O2 / Inert Atmospheres // AIAA JOURNAL. - 1972. - V. 10, No. 6. - P.776-783.

15. Maggi F., Bandera A., Galfetti L., De Luca LT, Jackson TL Efficient solid rocket propulsion for access to space // Acta Astronautica. - 2010. - V. 66. - P.1563-1573.

16. Liang D., Liu J., Zhou J., Wang Y., Yang Y. Combustion Characteristics and Propulsive Performance of Boron / Ammonium Perchlorate Mixtures in Microtubes // Journal of Energetic Materials. - 2016. - V. 34, No. 3. - P.297-317.

17. Galfetti L., De Luca LT, Severini F., Meda L., Marra G., Marchetti M., Regi M., Bellucci S. Nanoparticles for solid rocket propulsion // Journal of Physics: Condensed Matter. - 2006. - V. 18. - P.1991-2005.

18. Connell Jr. TL, Risha GA, Yetter RA, Roberts CW, Young G. Boron and Polytetrafluoroethylene as a Fuel Composition for Hybrid Rocket Applications // Journal of propulsion and power. - 2014. - V. 31, No. 1. P.373-385.

19. Liu PJ., Liu LL., He GQ. Effect of solid oxidizers on the thermal oxidation and combustion performance of amorphous boron. Journal of Thermal Analysis and Calorimetry. - 2016. - V. 124, I. 3. - P.1587-1593.

20. Abraham A., Nie H., Schoenitz M., Vorozhtsov AB, Lerner M., Pervikov A., Rodkevich N., Dreizin EL Bimetal Al-Ni nano-powders for energetic formulations // Combustion and Flame. - 2016. - V. 173. - P.179-186.

Figure 1. A.G. Korotkikh

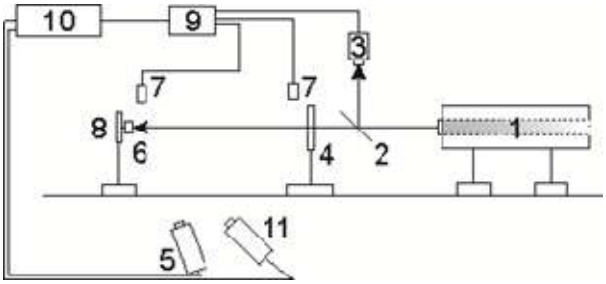

Fig. 1. Scheme of experimental setup based on CO_2-laser: 1 – CO_2-laser; 2 – semitransparent mirror; 3 – radiation power measurer; 4 – shutter; 5 – videocamera; 6 – HEM sample; 7 – photodiodes; 8 – sample holder; 9– ADC; 10 – PC; 11 – thermal imaging camera.

Figure 2. A.G. Korotkikh

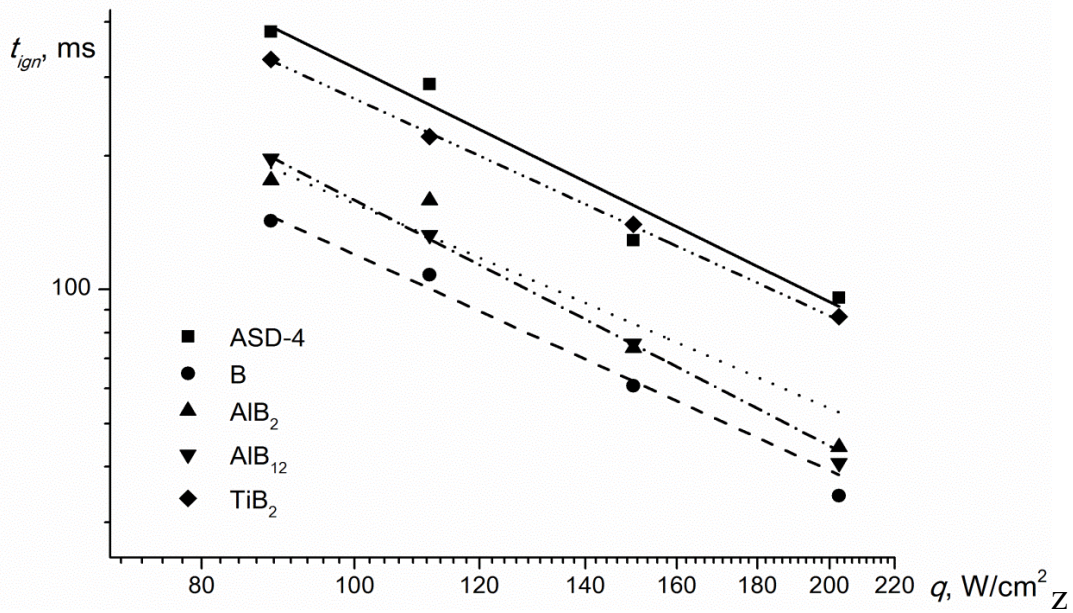

Fig.2 – Solid fuel ignition delay time vs laser heat flux density.

Figure 3. A.G. Korotkikh

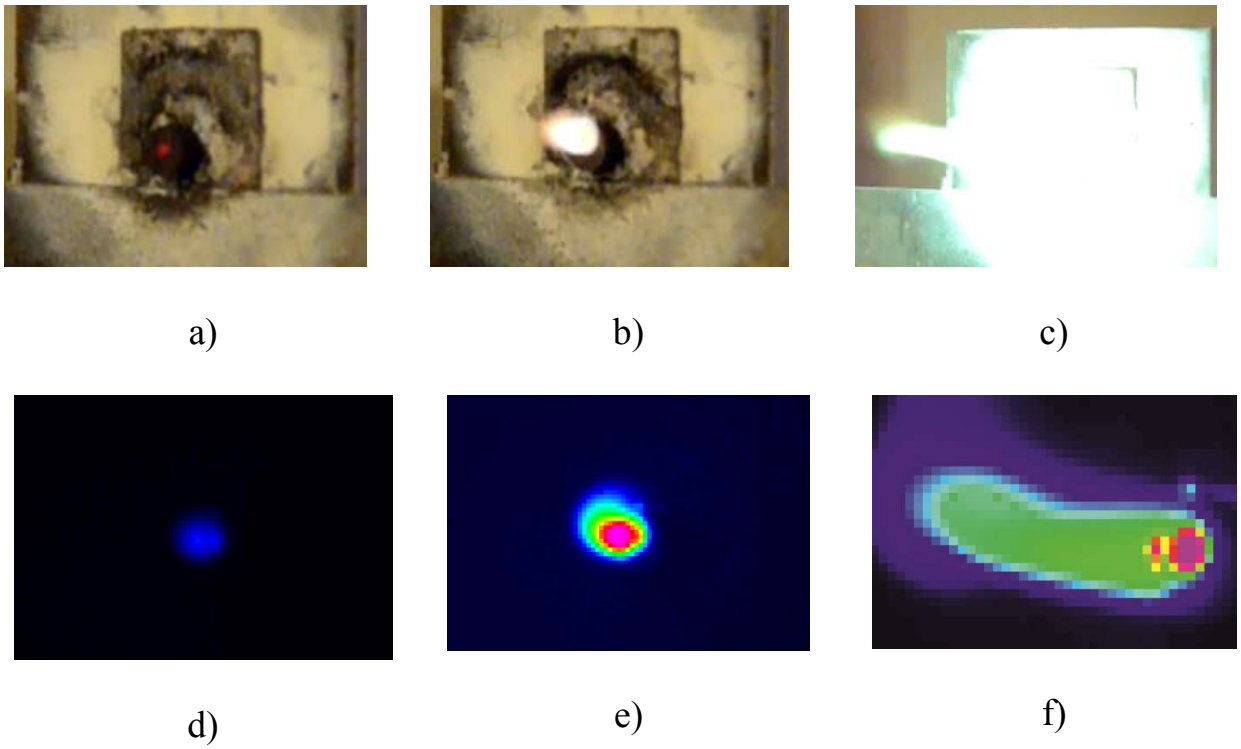

Fig.3 – Synchronized in time cadres of video and thermal-imaging camera for main stages of composite fuel ignition on the example of sample AlB_2: a, d – beginning of heating; b, e – heating stage; c, f – moment of ignition.

Figure 4. A.G. Korotkikh

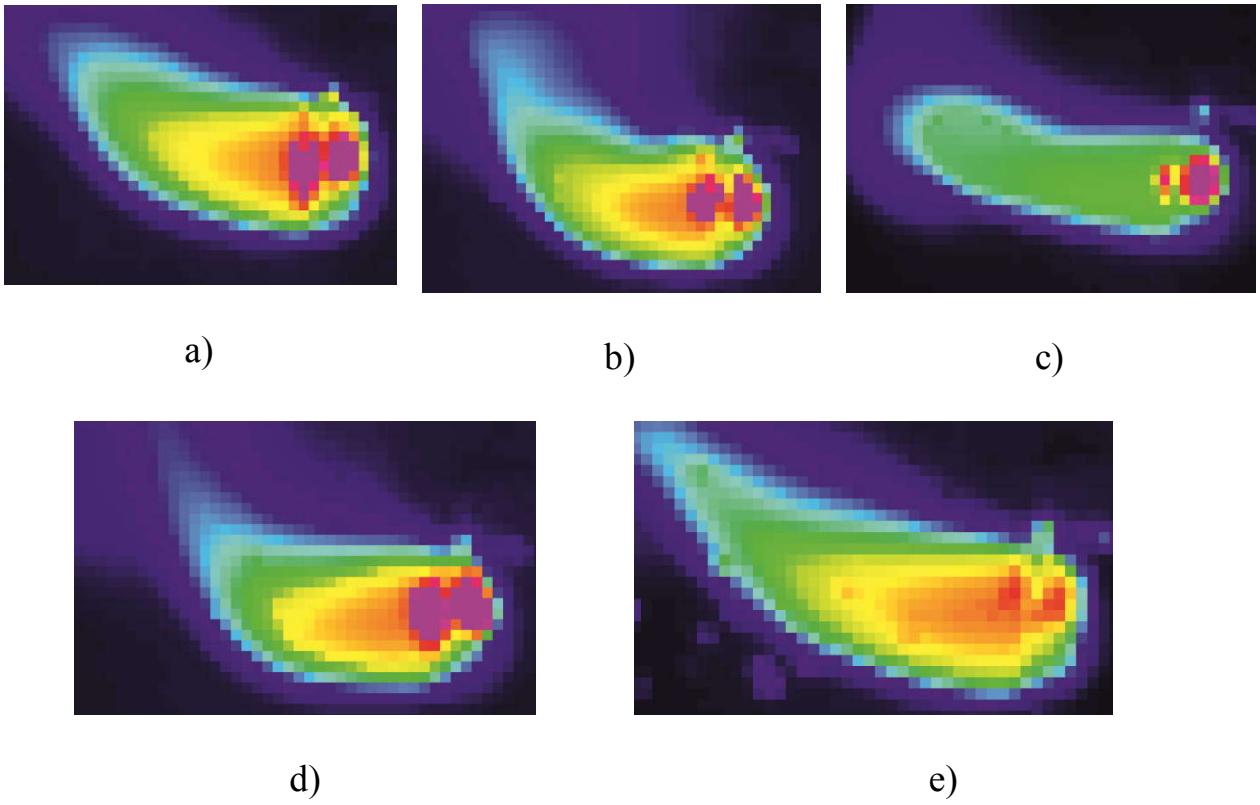

Fig. 4 – Temperature distribution on sample surface at moment of ignition for samples with: a – ASD-4; b – B; c – AlB_2; d – AlB_{12}; e – TiB_2.

Figure 5. A.G. Korotkikh

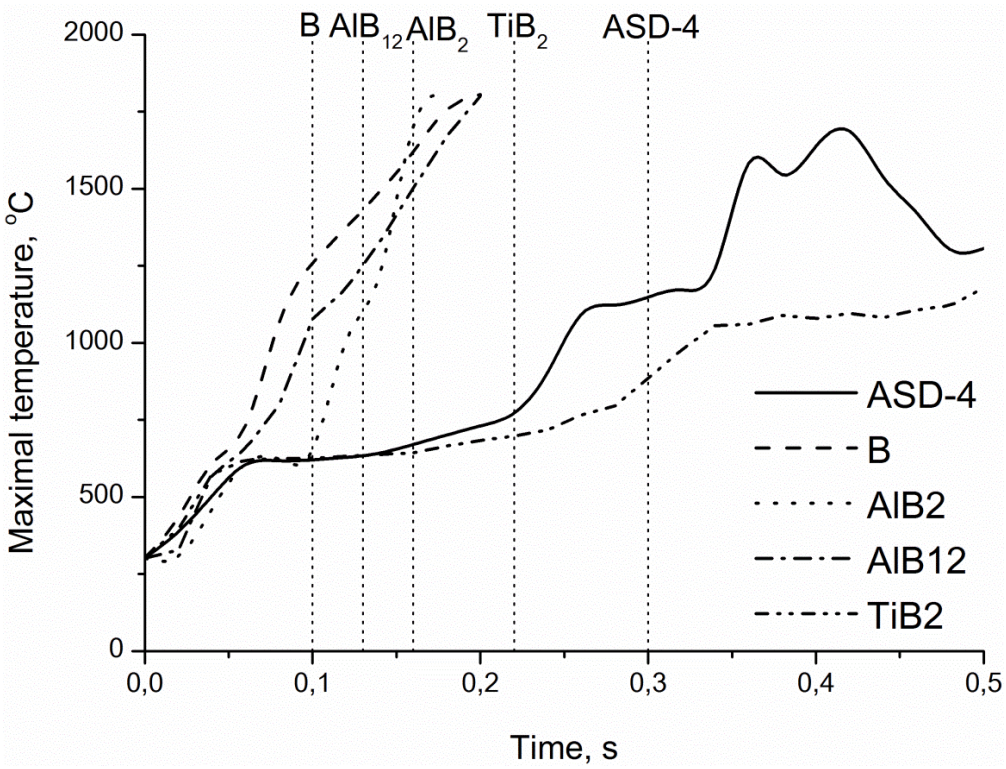

Fig. 5 – Maximal temperature of fuel sample surface vs time.

Figure 6. A.G. Korotkikh

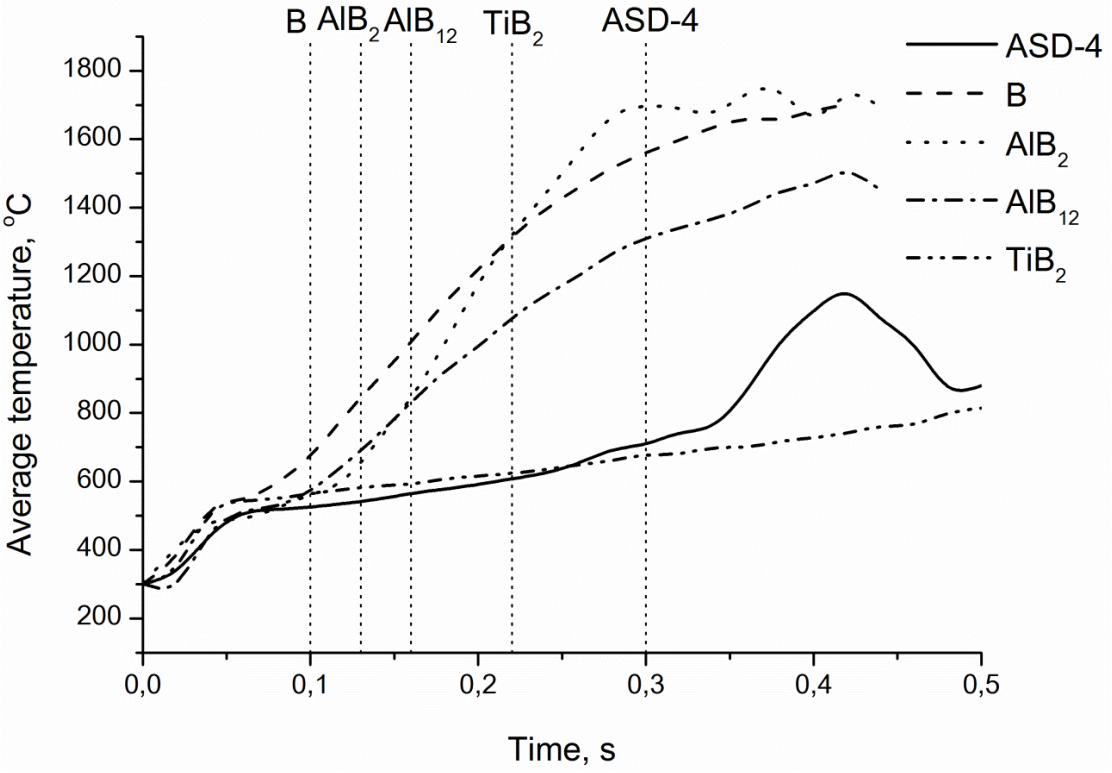

Fig. 6 – Average temperature of fuel sample surface vs time.

Table 1 – Approximation constant and determination coefficient values.

Sample	ASD-4	B	AlB_2	AlB_{12}	TiB_2
A	989939	202347	177596	739051	470896
B	1,748	1,614	1,528	1,834	1,622
R^2	0,9545	0,9818	0,8743	0,9983	0,9988

Table 2 – Sample surface characteristic temperatures at the moment of ignition

Samples	ASD-4	B	AlB_2	AlB_{12}	TiB_2
Surface maximal temperature, °C	1124	1258	1006	1176	683
Surface average temperature, °C	691	560	574	576	616

Table 3 – Activation energy and characteristic temperature values from calculation

Sample	ASD-4	B	AlB_2	AlB_{12}	TiB_2
E_a, kJ/моль	218,9	119,8	97,51	306,9	135,5
T*, °C	1686	1332	1744	1114	1939
T_2, °C	926	582	663	659	860
$Q_z\ 10^8$	$8.32\ 10^{10}$	$3.77\ 10^8$	0.051	$4.81\ 10^{18}$	$3.84\ 10^7$

Figure capture

Fig. 1. Scheme of experimental setup based on CO2-laser: 1 – CO2-laser; 2 – semitransparent mirror; 3 – radiation power measurer; 4 – shutter; 5 – videocamera; 6 – HEM sample; 7 – photodiodes; 8 – sample holder; 9– ADC; 10 – PC; 11 – thermal imaging camera.

Fig.2 – Solid fuel ignition delay time vs laser heat flux density.

Fig.3 – Synchronized in time cadres of video and thermal-imaging camera for main stages of composite fuel ignition on the example of sample AlB2: a, d – beginning of heating; b, e – heating stage; c, f – moment of ignition.

Fig. 4 – Temperature distribution on sample surface at moment of ignition for samples with: a – ASD-4; b – B; c – AlB2; d – AlB12; e – TiB2.

Fig. 5 – Maximal temperature of fuel sample surface vs time.

Fig. 6 – Average temperature of fuel sample surface vs time.